Synthesis, Activity, and Molecular Modeling of a New Series of Tricyclic Pyridazinones as Selective Aldose Reductase Inhibitors

Luca Costantino,[†] Giulio Rastelli,[†] Katia Vescovini,[†] Giorgio Cignarella,[‡] Paola Vianello,[‡] Antonella Del Corso,[§] Mario Cappiello,[§] Umberto Mura,[▽] and Daniela Barlocco*,[†]

Dipartimento di Scienze Farmaceutiche, Via G. Campi 183, 41100 Modena, Italy, Ist. Chim Farmaceutico e Tossicologico, Viale Abruzzi 42, 20131 Milano, Italy, Dipartimento di Fisiologia e Biochimica, Via S. Maria 55, 56100 Pisa, Italy, and Dipartimento di Scienze Biomediche, Via G. Campi 287, 41100 Modena, Italy

Three new series of tricyclic pyridazinones have been synthesized and tested *in vitro* in order to assess (i) their ability to inhibit aldose reductase enzyme (ALR2) and (ii) their specificity toward the target enzyme with respect to other related oxidoreductases, such as aldehyde reductase, sorbitol dehydrogenase, and glutathione reductase. The inhibitory capability of the most effective compounds (IC$_{50}$ values ranging from 6.44 to 12.6 μM) appears to be associated with a rather significant specificity for ALR2. Molecular mechanics and molecular dynamic calculations performed on the ALR2−inhibitor complex give indications of specific interaction sites responsible for the binding, thus providing information for the design of new inhibitors with improved affinity for the enzyme.

Introduction

Aldose reductase (alditol:NADP$^+$ oxidoreductase, EC 1.1.1.21, ALR2) is the first enzyme of the so-called "polyol pathway"; in the presence of NADPH it converts glucose to sorbitol, which is further processed by sorbitol dehydrogenase (L-iditol:NAD$^+$ 5-oxidoreductase, EC 1.1.1.14, SD) to fructose.[1] Since ALR2 has low affinity for glucose, flux through this pathway is probably low in most tissues under physiological conditions. However, under diabetic conditions, in tissues such as nerve, lens, and retina, in which insulin is not necessary for glucose transport across the membrane, glucose concentration increases sufficiently to provide a substrate for ALR2. The increased glucose flux through the sorbitol pathway and/or the high intracellular accumulation of sorbitol are likely to be involved in the etiology of late-onset diabetic complications such as neuropathy, nephropathy, retinopathy, and cataract.[1,2] Accordingly, suitable inhibitors of ALR2, developed by means of molecular modeling,[3−5] have been proposed as therapeutic agents capable of delaying the onset of long-term diabetic complications or minimizing their severity.[1,6]

However, several problems are associated with aldose reductase inhibitor (ARI) therapy. The first concerns the specificity of the inhibition: ALR2 is a member of the aldo−keto reductase family, a group of enzymes that catalyze the NADPH-dependent reduction of a wide variety of carbonyl compounds, possessing a broad and overlapping substrate specificity.[7] The possible consequences arising, in the course of chronic ARI therapy, from the inhibition of closely related enzymes not involved in the polyol pathway are therefore of legitimate concern in the development of any ARI. The highest homology in structure and activity is seen with aldehyde reductase (alcohol:NADP$^+$ oxidoreductase, EC 1.1.1.2, ALR1).[7] Even though the physiological role of this enzyme is not clear, it does not appear to participate significantly in polyol formation *in vivo*.[8]

Another problem associated with ARI therapy is the decline in effectiveness of the inhibitors over prolonged periods of treatment.[9] This could depend on the induction of drug metabolism or on the emergence of different enzyme forms less susceptible to inhibition.[9,10] This might be the case of glutathione-modified aldose reductase, an enzyme form generated in the lens under oxidative stress,[11] which displays a markedly reduced sensitivity to certain ARIs.[12]

The X-ray structure of ALR2 complexed with zopolrestat, a phthalazineacetic acid derivative, has recently been reported.[13] This study provides a useful interpretation of the inhibitory activity of closely related compounds. The observation that several potent ARIs (e.g., ponalrestat, zopolrestat, and analogs)[14,15] contain a pyridazine moiety, and the claim in a very recent paper[16] that a series of (4-carboxy-6-aryl-3-oxopyridazin-2-yl)acetic acids has weak ALR2 inhibitory activity, led us to examine the possibility of the previously described tricyclic pyridazinones **1**−**3**[17,18] as being a suitable substrate for the development of a new class of compounds provided with similar properties.

This paper reports on the synthesis of compounds **7**−**15** together with their *in vitro* ability to inhibit native aldose reductase and their selectivity with respect to other related enzymes displaying pyridine cofactor-dependent oxidoreductase activity.

SD and glutathione reductase (NADPH:glutathione oxidoreductase, EC 1.6.4.2, GR) were considered as potential targets for ARI action in addition to ALR1. Owing to its involvement in the polyol pathway, SD inhibition could significantly increase the cellular steady-state level of sorbitol, possibly eliminating ALR2 inhibition. On the other hand, the relevance of GR in determining the level of glutathione in the reduced state is well documented, and any drug-dependent impairment of GSSG/GSH recycling may cause oxidative damage to the cell.[19,20]

The unsubstituted-phenyl derivative **8aa** was therefore selected as a model for this class of compounds and

---

Chart 1

1-3

7-9

10-12

13-15

n, m = 1-3   R = H, OCH₃, CH₃

Zopolrestat

Ponalrestat

Scheme 1[a]

n = 1   **1**
n = 2   **2**
n = 3   **3**

a

b

n = 1   **4**
n = 2   **5**
n = 3   **6**

n = 1   **7**
n = 2   **8**
n = 3   **9**
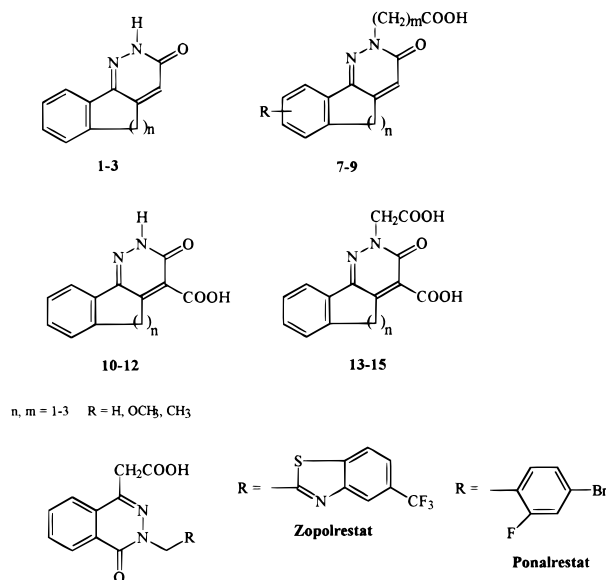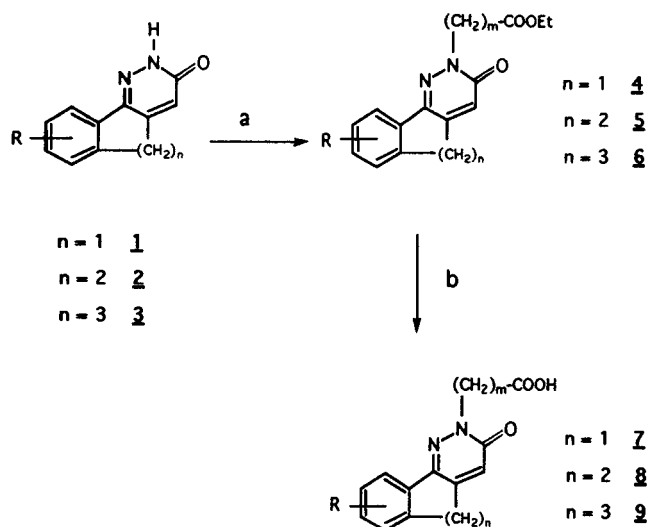
[a] (a) Br-$(CH_2)_m$-COOEt, K_2CO_3/acetone/Δ; (b) (1) NaOH/95% EtOH/rt, (2) HCl/Et₂O. R = H (**a**), $(OMe)_2$ (**b**), Me₂ (**c**).

docked into the experimentally determined structure of ALR2. The complexes were energy-minimized using molecular mechanics and further investigated by molecular dynamics simulations. The results indicate how this class of compounds might bind to the enzyme and provide insight for the design of more potent analogs.

Chemistry

Derivatives **7**–**9**, having a carboxylic acid in position 2, were prepared from the corresponding pyridazinones **1**–**3**[17,18] by treatment with the required ethyl bromoester to give the esters **4**–**6**, which are easily converted into **7**–**9** by alkaline hydrolysis (see Scheme 1). The 4,4a-dihydro derivative **16c** was similarly obtained from the corresponding dihydrobenzocinnolinone **21c**, in turn prepared from **20c**, according to standard procedures[18] (see Scheme 2).

The hitherto unknown dimethoxy- and dimethylbenzocinnolinones (**2b,c**) were prepared according to a previously reported method,[18] starting from 6,7-dimethoxy-1-tetralone and 5,7-dimethyl-1-tetralone

(**17b,c**), respectively. It is to be noted that, in the case of **17b**, the reaction with glyoxylic acid in alkaline medium yielded a remarkable amount of 2′-hydroxyacid **19b** in addition to the expected unsaturated acid **18b**, thus enabling us to obtain **2b** by direct condensation of **19b** with hydrazine hydrate in acetic acid (see Scheme 2).

Compounds **13**–**15**, having an additional carboxyl group in position 4, were synthesized by treating the required commercial ketones **23**–**25** with diethyl mesoxalate, according to Sing.[21] The resultant diesters **26**–**28** were cyclized either with hydrazine dihydrochloride in ethanol or with hydrazine hydrate in acetic acid to the corresponding **29**–**31**, which by nucleophilic substitution with ethyl bromoacetate led to the tricyclic diesters **32**–**34**, which were subsequently hydrolyzed in alkaline medium to the desired 2,4-disubstituted acids **13**–**15**. Finally, compounds **10**–**12**, lacking the acidic function in position 2, were easily obtained by alkaline hydrolysis of the intermediate corresponding esters **29**–**31** followed by acidification with 1 N hydrochloric acid.

Biological Assays

All the new compounds were studied *in vitro* for their ability to inhibit aldose reductase, sorbitol dehydrogenase, and two other enzymes, namely, aldehyde reductase and glutatione reductase, which are not involved in the polyol pathway. Moreover, the three most significant derivatives (**8bc,ca,cc**) were also investigated for their inhibitory activity towards modified aldose reductase forms. Sorbinil and tolrestat were used as reference compounds.

Results and Discussion

Biology. The effectiveness of this new series of tricyclic pyridazinones as inhibitors of ALR2 is summarized in Table 3, where the inhibitory effect of the compounds on ALR1, sorbitol dehydrogenase, and glutathione reductase is also reported. The most active ARIs derivatives (**8aa,ca,ac,bc**) (IC₅₀ values ranging from 6.44 to 12.6 μM), comparable to sorbinil (IC₅₀ = 3.04 μM) but less effective than inhibitors like ponalrestat and zopolrestat, which act in the nanomolar range, exhibit a significant selectivity for ALR2. In fact, much lower (**8ac,ca**) or no inhibition (**8bc,aa**) could be detected for SD or GR activities.

Of the homologous 2-substituted acetic acid derivatives (**7**–**9**, R = H; Table 1) benzocinnolinone **8aa** exhibited the most interesting properties, having IC₅₀ = 12.6 μM. The higher homolog **9aa** was 6 times less active (IC₅₀ = 76.2 μM), while the lower analog **7aa** was only slightly active (35.8% inhibition at 158 μM). Introduction of two methoxy groups on the phenyl ring of **8aa** (compound **8ba**) led to a less active derivative (IC₅₀ = 114 μM), while the same substituents greatly improved the inhibitory properties of the lower homolog **7ba** (IC₅₀ = 26.4 μM). On the other hand, introduction of two methyl groups on the phenyl ring of **8aa** led to a more active compound (**8ca**, IC₅₀ = 6.44 μM), whose properties were badly affected by reduction of the 4,4a-double bond (compound **16c**, IC₅₀ = 63.5 μM). Introduction of an additional carboxy group in position 4 of the pyridazinonic ring in all cases led to less active derivatives (**13**–**15**). Elongation of the acetic acid moiety by one methylene decreased the activity of both the un-
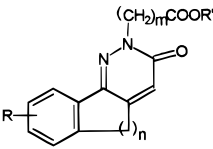
Scheme 2[a]

R = 6,7-(OMe)$_2$ **b**

R = 5,7-Me$_2$ **c**
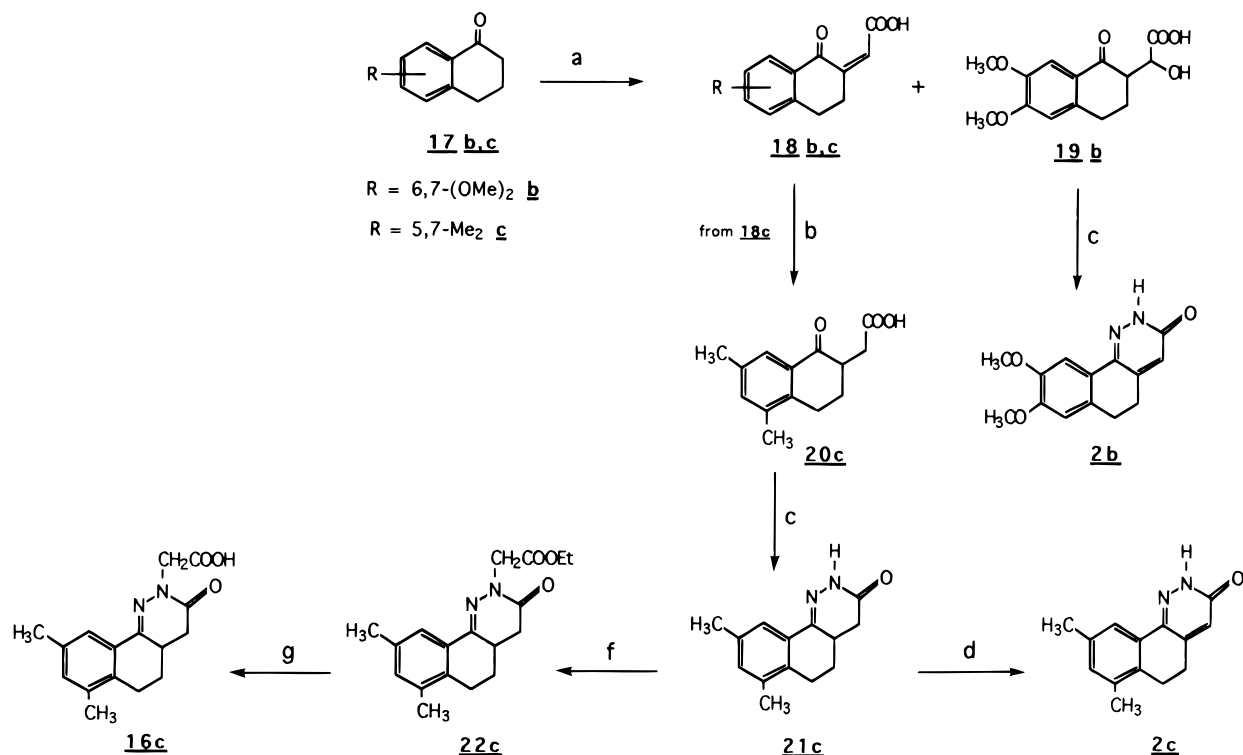
[a] (a) Glyoxylic acid/OH$^-$/Δ; (b) Zn/CH$_3$COOH/Δ; (c) NH$_2$-NH$_2$·H$_2$O/EtOH/Δ; (d) *m*-nitrobenzensulfonate/OH$^-$; (e) NH$_2$-NH$_2$·H$_2$O/CH$_3$COOH/Δ; (f) Br-CH$_2$COOEt/K$_2$CO$_3$/acetone/Δ; (g) (1) NaOH/95% EtOH/Δ, (2) HCl/Et$_2$O.

Scheme 3[a]
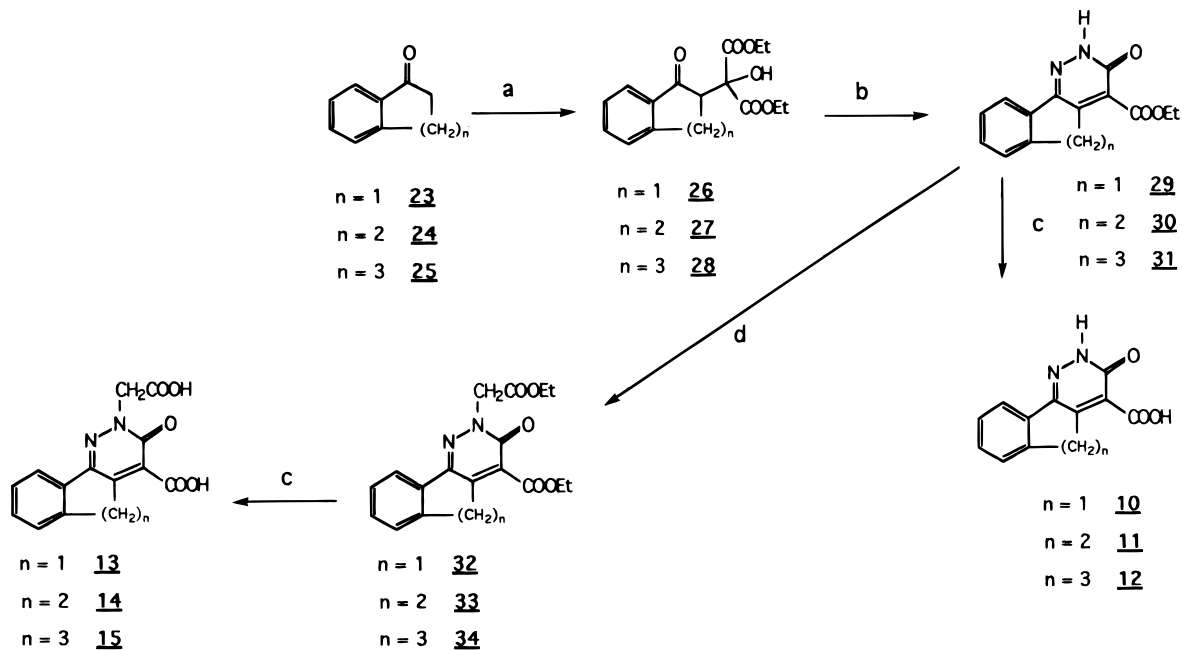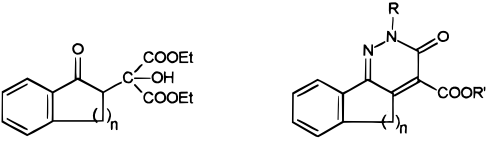
[a] (a) Diethyl mesoxalate/Δ; (b) NH$_2$-NH$_2$·2HCl/EtOH/Δ or NH$_2$-NH$_2$·H$_2$O/CH$_3$COOH/Δ; (c) NaOH/EtOH/H$_2$O; (d) BrCH$_2$COOEt/K$_2$CO$_3$/acetone/Δ.

substituted (**8ab**) and the substituted (**8bb,cb**) benzocinnolinones. On the other hand, further elongation to butyric acid derivatives gave different results, depending on the substrate. In fact, in the case of the unsubstituted derivatives, the transition from the acetic acid (**8aa**) to the butyric acid (**8ac**) derivative did not cause any apparent difference (IC$_{50}$ = 12.6 vs 11.4 μM), while the dimethyl-substituted butyric acid derivative **8cc** was slightly less active than the corresponding acetic acid derivative **8ca** (IC$_{50}$ = 17.4 vs 6.44 μM). The

most intriguing result was found in the case of the dimethoxy-substituted derivatives, where introduction of a butyric acid substituent (**8bc**) instead of an acetic acid residue (**8ba**) brought about an almost 15-fold increase in inhibitory activity (IC$_{50}$ = 7.56 vs 114 μM). The importance of the carboxylic function in the inhibition of ALR2 is underlined by the fact that in all cases its esterification led to less active derivatives (**5ba**, 21% inhibition at 101 μM; **5bc**, 35% inhibition at 79 μM; **5ca**, 31% inhibition at 48 μM). Finally, it should be noted

Table 1. Physicochemical Data of Compounds **5** and **7**−**9**

compd	n	m	R	R′	% yield	mp, °C	formula
5ba	2	1	8,9-(OMe)$_2$	Et	90	142−143	C$_{18}$H$_{20}$N$_2$O$_5$
5ca	2	1	7,9-Me$_2$	Et	88		C$_{18}$H$_{20}$N$_2$O$_3$
5cb	2	2	7,9-Me$_2$	Et	80		C$_{19}$H$_{22}$N$_2$O$_3$
5bc	2	3	8,9-(OMe)$_2$	Et	75	82−83	C$_{20}$H$_{24}$N$_2$O$_5$
5cc	2	3	7,9-Me$_2$	Et	83	86−87	C$_{20}$H$_{24}$N$_2$O$_3$
7aa	1	1	H	H	35	165−68	C$_{13}$H$_{10}$N$_2$O$_3$
7ba	1	1	7,8-(OMe)$_2$	H	45	180−82	C$_{15}$H$_{14}$N$_2$O$_5$
8aa	2	1	H	H	42	225−28	C$_{14}$H$_{12}$N$_2$O$_3$
8ba	2	1	8,9-(OMe)$_2$	H	80	198−200	C$_{15}$H$_{16}$N$_2$O$_5$
8ca	2	1	7,9-Me$_2$	H	85	210−12	C$_{15}$H$_{16}$N$_2$O$_3$
8ab	2	2	H	H	70	224−25	C$_{15}$H$_{14}$N$_2$O$_3$
8bb	2	2	8,9-(OMe)$_2$	H	55	177−178	C$_{16}$H$_{18}$N$_2$O$_5$
8cb	2	2	7,9-Me$_2$	H	50	162−65	C$_{16}$H$_{18}$N$_2$O$_3$
8ac	2	3	H	H	50	168−70	C$_{16}$H$_{16}$N$_2$O$_3$
8bc	2	3	8,9-(OMe)$_2$	H	80	149−150	C$_{17}$H$_{20}$N$_2$O$_5$
8cc	2	3	7,9-Me$_2$	H	71	228−229	C$_{17}$H$_{20}$N$_2$O$_3$
9aa	3	1	H	H	53	208−10	C$_{15}$H$_{14}$N$_2$O$_3$

Table 2. Chemical Data of Compounds **10**−**15** and Their Precursors **26**−**31**

compd	n	R	R′	% yield	mp, °C	formula
10	1	H	H	50	>230	C$_{12}$H$_8$N$_2$O$_3$
11	2	H	H	38	210−12	C$_{13}$H$_{10}$N$_2$O$_3$
12	3	H	H	35	210−13	C$_{14}$H$_{12}$N$_2$O$_3$
13	1	CH$_2$COOH	H	70	218−20	C$_{14}$H$_{10}$N$_2$O$_5$
14	2	CH$_2$COOH	H	50	180−83	C$_{15}$H$_{12}$N$_2$O$_5$
15	3	CH$_2$COOH	H	45	200	C$_{16}$H$_{14}$N$_2$O$_5$
26	1			82	79−80	C$_{16}$H$_{18}$O$_6$
27	2			70	52−53	C$_{17}$H$_{20}$O$_6$
28	3			75	oil	C$_{18}$H$_{22}$O$_6$
29	1	H	Et	63		C$_{14}$H$_{12}$N$_2$O$_3$
30	2	H	Et	45	231−34	C$_{15}$H$_{14}$N$_2$O$_3$
31	3	H	Et	40		C$_{16}$H$_{16}$N$_2$O$_3$

that the presence of the acidic function in position 2 of the pyridazinonic ring is an essential requirement for activity, as indicated by the complete inactivity of compounds **10**−**12**, which lack this substituent but retain the carboxylic group in position 4.

The effectiveness of some of the most active synthesized compounds, such as **8ca**,**bc**,**cc**, was tested on pure native ALR2, and the results obtained with the partially purified enzyme were confirmed. The kinetic analysis of inhibition, performed on **8ca** with pure native ALR2, reveals a noncompetitive type of action with respect to both substrate and cofactor, with apparent inhibition constants of 2.3 ± 0.5 and 2.8 ± 0.3 μM. Despite the occurrence of a noncompetitive type of action, as judged by steady-state kinetic analysis, the molecular modeling approach (see below) assumes and actually supports a direct interaction of the inhibitors at the active site of ALR2. This apparent anomaly is common to other ARIs, which behave as non- or uncompetitive inhibitors when tested in the direction of aldehyde reduction. It has been suggested[22] that lack of competitive inhibition
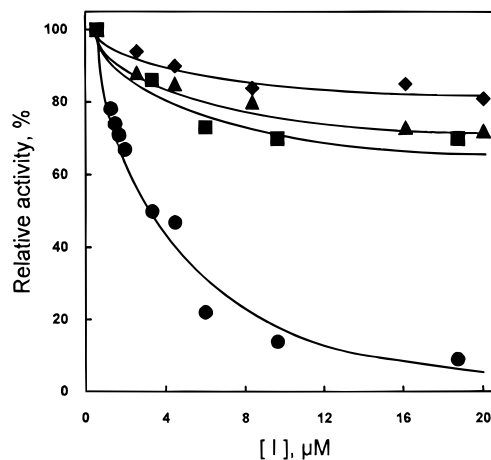

Figure 1. Effect of compound **8ca** on the activity of native and thiol-modified forms of aldose reductase. Native aldose reductase (●) and glutathione-modified (■), carboxymethylated (▲), and 2-mercaptoethanol-modified (♦) forms of aldose reductase were incubated as described in the Experimental Section in the presence of various concentrations of compound **8ca**. Residual activities are expressed as percentage of activity measured in the absence of the inhibitor; 100% = 2 mU in the assay.

does not exclude the possibility of an inhibitor binding at the substrate binding site of ALR2; in the case of at least two inhibitors, citrate and zopolrestat, direct evidence for active site binding has been obtained by crystallographic analysis.[13,23] A satisfactory model for the explanation of the phenomenon has recently been proposed on the basis of the peculiar mechanism of action of the enzyme.[24] As has previously been observed for sorbinil,[12,25−27] there is a dramatic loss of sensitivity to inhibition by the tested compounds when ALR2 is modified at the level of Cys298. Thus, the above active ARIs had no effect on ALR2 in which Cys298 was modified either by carboxymethylation or by thiolation with glutathione or 2-mercaptoethanol. The effect of **8ca** on the pure native ALR2 and on the three different modified enzyme forms is shown in Figure 1.

Molecular Modeling. A common structural feature of many ARIs is a carboxylate functional group. Wilson *et al.*[13] recently reported a refined 1.8 Å structure of human aldose reductase complexed with zopolrestat, one of such carboxylic acid inhibitors. Further findings led researchers to postulate an anion binding site particularly suitable for the binding of carboxylates and constituted by Tyr48, His110, and the nicotinamide ring of NADP$^+$.[23] With the aim of defining the interaction sites between ALR2 and the test compounds, the phenyl-unsubstituted derivative **8aa,** one of the most potent inhibitors here described, was docked, as a model compound, into the crystal structure of human ALR2.[28] To this end, the enzyme−inhibitor complex was energy-minimized with molecular mechanics. (See Computational Procedure in the Experimental Section.)

Figure 2 reports a selection of residues interacting with the inhibitor in the minimized complex. The carboxylate is electrostatically attracted by the positive nicotinamide ring of NADP$^+$ and is strongly held in place by three hydrogen bonds with Tyr48, His110, and Trp111. The carbonyl group of the pyridazinone is hydrogen-bonded with Cys298. The hydrophobic portion of the inhibitor points toward the mouth of the cavity and makes favorable contacts with Trp20, Trp219,

Table 3. Enzyme Inhibition Data[a]

compd	aldose red	aldehyde red	sorbitol dehydr	glutathione red
7aa	35.8% (158 μM)	107 (74.1−155)	b	9.4% (211 μM)
7ba	26.4 (24.9−28.1)	44.1% (163 μM)	b	11.2% (149 μM)
8aa	12.6 (7.14−22.1)	156 (141−173)	b	4.2% (138 μM)
8ba	114 (60.8−215)	11.3% (132 μM)	b	b
8ca	6.44 (2.09−19.8)	295 (214−409)	b	b
8ab	133 (117−152)	32.7% (152 μM)	b	b
8bb	162 (118−222)	8.0% (126 μM)	b	b
8cb	51.5 (46.1−57.5)	289 (243−343)	b	b
8ac	11.4 (7.60−17.2)	92.6 (65.8−130)	b	b
8bc	7.56 (3.50−16.3)	10.1% (112 μM)	b	b
8cc	17.4 (13.9−21.8)	22.1% (141 μM)	b	b
9aa	76.2 (50.4−115)	15.1% (143 μM)	b	b
10	5.3% (143 μM)	0% (197 μM)	b	12.3% (191 μM)
11	9.9% (131 μM)	8.3% (152 μM)	b	18.9% (175 μM)
12	13.2% (125 μM)	6.8% (189 μM)	b	b
13	32.4% (57 μM)	136 (77.8−238)	b	22.3% (152 μM)
14	33.0 (26.5−41.0)	161 (128−203)	b	23.7% (148 μM)
15	12.1% (92 μM)	10.3% (128 μM)	b	b
16c	63.5 (53.3−75.7)	21.8% (141 μM)	b	b
sorbinil	3.04 (2.91−3.52)	1.74 (1.69−1.79)	b	b
tolrestat	0.096 (0.079−0.117)	1.21 (0.87−1.70)	16.4% (120 μM)	b
quercetin	39.9 (28.3−56.1)	10.3 (5.91−18.1)	177 (160−197)	218 (208−228)

[a] IC$_{50}$ (95% CL) (μM) or percent inhibition (at a given μM concentration). [b] No inhibition was observed up to 150 μM of the test compound.
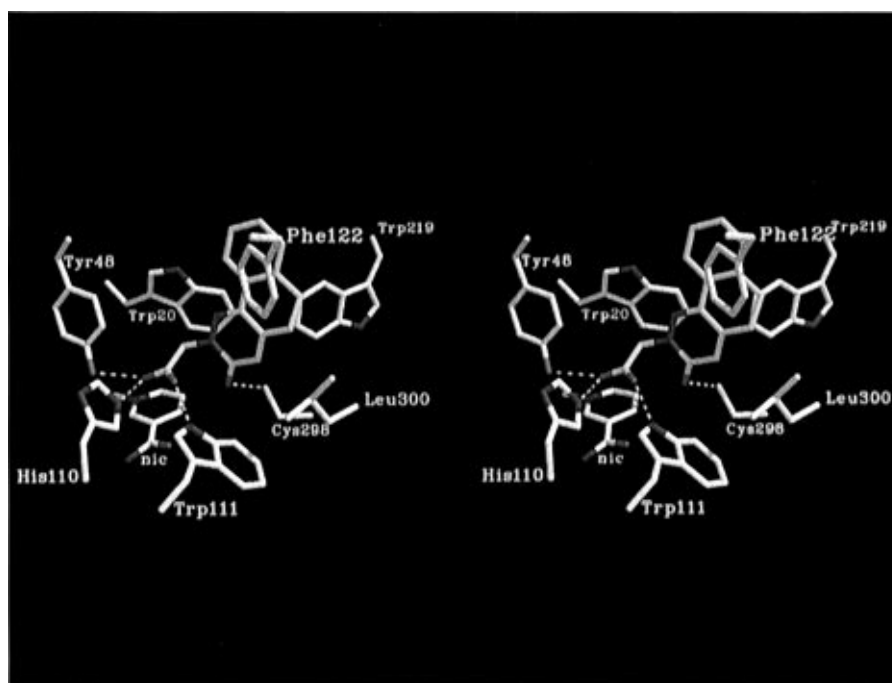

Figure 2. Selection of residues interacting with the inhibitor **8aa** (yellow) in the structure of the minimized complex with ALR2 (cross-eyed stereopicture). Hydrogen bonds with Tyr48, His110, Trp111, and Cys298 are drawn as dashed lines.

Phe122, and Leu300. Trp20 and Phe122 are similarly involved in hydrophobic contacts with the phthalazinone ring of zopolrestat in the crystal structure of its complex with ALR2,[13] while Leu300 interacts with the benzothiazole of the inhibitor. Trp219 is not directly involved in the binding of zopolrestat. All residues so far mentioned are conserved in human, bovine, and porcine ALR2 sequences. It is worth mentioning that the inhibitor hydrogen bonds two very important residues in catalysis, i.e., Tyr48 and His110. The former residue is the proton donor during aldehyde reduction; the latter is important for a proper orientation of substrates.[29] The hydrogen bond with Cys298 might also be of relevance; not only has this residue been found to affect NADPH and substrate binding,[30] it is also potentially involved in modifications of the enzyme occurring under conditions that cause cellular oxidative damage.[11,31] Actually, the possible generation of glutathione-modified ALR2, an enzyme form which, owing to structural and kinetic differences with respect to the native ALR2,[12] is confirmed as being rather insensitive to inhibition (Figure 1), should be taken into account in the definition of strategies devoted to inhibit ALR2 activity.

In the crystal structure of the zopolrestat−ALR2 complex, the binding of the inhibitor was found to cause fairly substantial conformational changes in the structure of the apoenzyme.[13] In order to gain insight into which parts of the binding site are flexible and which are rigid in the presence of our inhibitor, we also performed molecular dynamics (MD) at 300 K, starting from the minimized complex. The MD simulations highlight a substantial motion of loop 116−133 and

Table 4. Root-Mean-Square Deviations (rms) of the Calculated Complex of **8aa** with ALR2 with Respect to the Holoenzyme and Interaction Energies (kcal/mol) between the Inhibitor and Some Selected (4 Å) Protein Residues

	rms		ΔE_{int}									
	loop 116−133	segment 298−308	Tyr48	His110	Trp111	Trp20	Phe122	Trp219	Cys298	Leu300	Trp79	Val47
minimized complex	0.29	0.22	−14.8	−17.7	−14.2	−6.0	−3.8	−3.7	−6.1	−1.9	−1.7	−2.8
10 ps	0.47	0.25	−14.8	−18.0	−13.7	−5.6	−4.8	−2.7	0.4	−2.6	−2.3	−4.5
20 ps	0.51	0.21	−15.4	−18.0	−14.2	−6.6	−4.4	−2.8	0.0	−1.6	−2.0	−4.6
50 ps	0.62	0.48	−14.8	−17.4	−14.8	−6.5	−1.9	−2.3	−6.5	−0.7	−2.4	−4.5
70 ps	0.58	0.62	−15.1	−17.2	−15.9	−4.8	−1.5	−0.4	−6.1	−0.5	−3.7	−4.6
100 ps	0.60	0.52	−14.7	−16.3	−15.3	−5.8		−0.4	−5.1	−0.2	−3.9	−4.8
180 ps	1.13	0.50	−14.2	−17.6	−13.9	−7.9		−2.4	−6.7	−1.0	−1.2	−3.3

segment 298−308. This finding is in agreement with the high average thermal motion (*B*-factors) observed for this loop both in the apoenzyme crystal structure[28] and in the zopolrestat-bound structure.[13]

In the minimized complex, loop 116−133 moves toward the pocket in a similar way as it moves to accommodate and sequester zopolrestat.[13] However, molecular dynamics gradually force loop 116−133 apart from segment 298−308 to form an open cavity. These displacements are drawn in Figure 3, and the deviation indices (rms) at various MD times are reported in Table 4. At 180 ps (Figure 3, blue line), loop 116−133 is almost in the open conformation. The high flexibility of this loop, as indicated by both MD and *B*-factors, suggests that there may be an equilibrium between a closed and an open form of this loop, the closed form being important to sequester hydrophobic substituents like the benzothiazolyl moiety of zopolrestat. This does not necessarily mean that the whole loop-opening/closing process can be followed by MD because the barriers may be too large and the simulations involved may take too long. Nevertheless, the MD calculations are able to indicate conformational flexibility in particular regions of the enzymes that tie in nicely with temperature factors, a finding which has already been observed for other proteins.[32−34]

The interaction energies of the inhibitor with the nearby protein residues (4 Å) are reported in Table 4. The most important interactions are with Tyr48, His110, and Trp111; analysis of the interaction energies at different times selected during the 180 ps MD also reveals that the inhibitor is able to maintain all of the critical binding interactions with the enzyme except for Phe122, which moves far away owing to the movement of loop 116−133. Furthermore, the interaction energies with Cys298 at 10 and 20 ps are significantly lower than at different MD times, since the mercapto hydrogen of Cys298 hydrogen bonds Tyr209; nevertheless, the hydrogen bond between the SH group of Cys298 and the carbonyl of the inhibitor is fully restored after 20 ps. The relevance of the Cys298−ARI interaction is confirmed by the loss of inhibitory activity caused by the derivatization on the Cys298 mercapto group by species quite different in sterical hindrance and charge (e.g., glutathione, β-mercaptoethanol, carboxymethylation).

The results obtained for compound **8aa** in the present simulation can help to understand the inhibitory activity of the other compounds reported here as well as to suggest new structures for synthesis and testing. The side chain of Trp20 fits in the binding cavity in such a way that a methylene bridge interposed between the carboxylate and the bulky portion of the inhibitor is required to allow the optimal interactions of the former
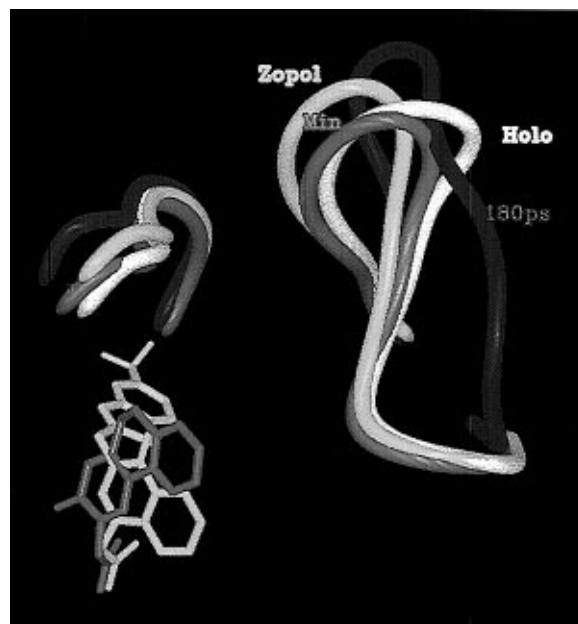

Figure 3. Conformational changes (α carbons) observed for loop minimization (red) and 180 ps dynamics (blue). The conformations assumed by the holoenzyme (white) and the zopolrestat-bound enzyme (yellow) can be inferred from the picture.

with Tyr48, His110, and Trp111 and, at the same time, to avoid steric repulsion of the latter with the enzyme (Figure 2); compounds possessing only one carboxylate directly attached at position 4 of the pyridazinone (compounds **10−12**) are completely inactive, even though there is a good chance, judging by model-built compounds rigidly docked into AR, that the interposition of the methylenic bridge even at position 4 could restore the favorable interactions observed for **8aa**. As regards the effects of substituents on the phenyl ring of **8aa,** they are not easy to explain on the basis of the structures here reported. The phenyl ring points toward the mouth of the binding cavity; the substituents would therefore be mainly exposed to solvent. It is possible that local changes in the distribution of water molecules around the phenyl ring and the nearby residues, particularly for the methoxy-substituted compound **8ba**, or global changes in the dipole moment of the inhibitor, could account for the observed trend in activity.

Finally, superimposing the structures of **8aa** on zopolrestat bound to ALR2 (Figure 4) leads one to speculate that position 4 of the pyridazinone can be functionalized with hydrophobic residues similar to the benzothiazolyl moiety of zopolrestat, in order to improve the binding of our inhibitors with the enzyme.
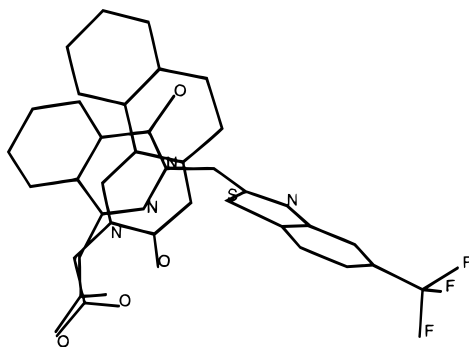
Figure 4. Superimposition of the structures of **8aa** with zopolrestat bound to ALR2.

Experimental Section

Chemistry. Melting points were determined on a Büchi 510 capillary melting point apparatus and are uncorrected. Elemental analyses for the test compounds were within ±0.4% of the theoretical values. ^{1}H-NMR spectra were recorded on a Brüker AC200 spectrometer; chemical shifts are reported as δ (ppm) relative to tetramethylsilane as internal standard. DMSO-d_6 was used as the solvent, unless otherwise noted. TLC on silica gel plates was used to check product purity. Silica gel 60 (Merck; 70−230 mesh) was used for column chromatography. Tolrestat was synthesized according to a procedure reported in the literature.[35] Sorbinil was kindly provided by Pfizer Inc. The structures of all compounds were consistent with their analytical and spectroscopic data.

Tricyclic Pyridazin-3(2H)-one-2-aliphatic Acids 7−9. General Method. (a) A mixture of the required pyridazinone **1−3** (0.01 mol),[17,18] the appropriate ethyl bromo ester (0.02 mol), and potassium carbonate (0.02 mol) in acetone (40 mL) was refluxed overnight. After cooling, the inorganic salts were filtered off, the solvent was evaporated, and the esters **4−6** were used for the next step without further purification. When necessary, a sample was purified by trituration with diethyl ether.

(b) A mixture of the appropriate ester **4−6** (0.01 mol) and sodium hydroxide (0.04 mol) in 95% ethanol (40 mL) was stirred at room temperature for 2 h. After evaporation of the solvent, the residue was acidified with hydrochloric acid in diethyl ether, diluted with water (20 mL), and extracted with dichloromethane (3 × 10 mL). After drying (Na₂SO₄) and evaporation of the solvent, the residue was crystallized from ethanol. (See Table 1 for chemical data.)

Tricyclic 4-Carboxypyridazin-3(2H)-one-2-acetic Acids 13−15. General Method. (a) A mixture of the required ketone **23−25** (0.01 mol) and diethyl mesoxalate (0.012 mol) was heated at 100 °C overnight. After cooling, the residue was purified by silica gel chromatography, eluting with cyclohexane/ethyl acetate (8/2), to give the desired **26−28**. In the case of **26**, we were able to purify the compound by crystallization from ethanol rather then by chromatography. (See Table 2 for chemical data.)

(b) A mixture of the required diester **26−28** (0.01 mol) and hydrazine dihydrochloride (0.01 mol) in ethanol (60 mL) was refluxed for 24 h. After cooling, when starting from **26**, a solid precipitated which was filtered by suction and thoroughly washed with ethanol to give **29**. In the case of the higher homologs **27** and **28**, the solvent was evaporated and the residue brought to pH 7 with 5% sodium bicarbonate and extracted with dichloromethane (3 × 30 mL). After drying (Na₂SO₄) and evaporation of the solvent, **30** and **31** were isolated in a second run by silica gel chromatography, eluting with dichloromethane/methanol (95/5); the first run yielded unreacted ketone. It should, however, be noted that, when starting from **27** and **28**, better yields were obtained if cyclization was carried out with hydrazine monohydrate in refluxing acetic acid for 12 h. Compounds were then isolated following the above reported workup. (See Table 2 for data.)

(c) A mixture of the appropriate **29−31** (0.01 mol), ethyl bromoacetate (0.01 mol), and potassium carbonate (0.01 mol)

in acetone (50 mL) was stirred at 40 °C for 3 h. The inorganic salts were filtered off, the solvent was evaporated, the resultant diesters **32−34** were directly suspended in 95% ethanol (50 mL), and sodium hydroxide (0.05 mol) was added. The mixture was then refluxed for 1 h and, after usual workup, yielded **13−15**. (See Table 2 for data.) However, it should be noted that in the case of **13** a better procedure was devised; sodium ethylate (0.0004 mol) was added portionwise to a mixture of **29** (0.1 g, 0.0004 mol) and ethyl bromoacetate (0.04 mL, 0.0004 mol) in toluene (2 mL) and the mixture heated at 60 °C for 2 h. After cooling and filtering off the inorganic salts, the solvent was evaporated and the residue purified by silica gel chromatography (dichloromethane/ethyl acetate, 7/3) to give 0.05 g (37%) of **32**. Hydrolysis to **13** was then performed by refluxing for 1 h in 4 N hydrochloric acid (5 mL).

Tricyclic 4-Carboxypyridazin-3(2H)-ones 10−12. General method. Compounds were prepared by alkaline hydrolysis, followed by acidification with hydrochloric acid in diethyl ether, of the appropriate **29−31**, as reported above for **7−9**. (See Table 2 for data.)

8,9-Dimethoxy-5,6-dihydrobenzo[h]cinnolin-3(2H)-one (2b). A solution of sodium hydroxide (1.9 g, 0.05 mol) in water (27 mL) and ethanol (14 mL) was added dropwise to an ice-cooled mixture of 6,7-dimethoxytetralone (**17b**) (2 g, 0.0097 mol) and glyoxylic acid (3.6 g, 0.04 mol) in water (16 mL), the temperature being kept below 15 °C. After stirring for 1 h at room temperature and refluxing for a further 3 h, the ethanol was evaporated and the mixture acidified with cooling to pH 2 using 30% hydrochloric acid. The resultant precipitate, consisting of a 40/60 mixture of **18b** and **19b**, as clearly indicated by ^{1}H-NMR spectroscopy, was directly cyclized by refluxing with hydrazine hydrate (0.95 g, 0.019 mol) in acetic acid (3 mL) for 4 h. After evaporation of the solvent, the residue was extracted with dichloromethane (3 × 5 mL) and repeatedly washed with 5% sodium bicarbonate to eliminate the unreacted **18b**. After drying (Na₂SO₄), the solvent was evaporated to give the desired **2b** as a yellow solid: yield 40% (from tetralone); mp = 200−205 °C; ^{1}H-NMR δ 2.9 (s, 4H), 3.9 (s, 6H), 6.9 (s, 1H), 7.0 (s, 1H), 7.5 (s, 1H), 12.9 (s, 1H, exch with D₂O).

7,9-Dimethyl-5,6-dihydrobenzo[h]cinnolin-3(2H)-one (2c). (a) A solution of sodium hydroxide (11.48 g, 0.29 mol) in water (160 mL) and ethanol (80 mL) was added dropwise to an ice-cooled mixture of 5,7-dimethyltetralone (**17c**) (10 g, 0.057 mol) and glyoxylic acid (21.1 g, 0.23 mol) in water (80 mL), the temperature being kept at around 15 °C. The mixture was then refluxed for 4 h. After evaporation of the solvent and dilution with water (30 mL), the mixture was extracted with dichloromethane (3 × 10 mL) to remove the unreacted tetralone and the aqueous layer acidified to pH 2 by 4 N hydrochloric acid. The resultant precipitate was filtered by suction to give 11.1 g (84%) of **18c**: mp = 179−180 °C; ^{1}H-NMR δ 2.2 (2s, 6H), 2.4−3.4 (m, 4H), 6.0 (br s, 1H, exch with D₂O), 6.8 (s, 1H), 7.2 (s, 1H), 7.8 (s, 1H).

(b) A mixture of **18c** (7 g, 0.03 mol) and zinc dust (3.6 g, 0.05 mol) in acetic acid (50 mL) was heated at 100 °C for 1 h. The salts were filtered off, the solvent was evaporated under vacuum, and the residue was mixed with hydrazine hydrate (2.3 g, 0.047 mol) and ethanol (50 mL) and refluxed for 3 h. After cooling, the precipitate was filtered by suction and triturated with diethyl ether to give 3 g (55%) of **21c**: mp = 205−207 °C dec; ^{1}H-NMR δ 2.2 (2s, 6H), 2.3−3.0 (m, 6H), 7.0 (s, 1H), 7.8 (s, 1H), 8.6 (br s, 1H, exch with D₂O).

(c) The 4,4a-dihydro derivative **21c** was transformed into **2c** by a standard procedure,[18] using sodium *m*-nitrobenzenesulfonate in alkaline medium: yield 85%; mp = 133−135 °C; ^{1}H-NMR (DMSO-d_6) δ 2.1 (2s, 6H), 2.8 (s, 4H), 6.8 (s, 1H), 7.1 (s, 1H), 7.6 (s, 1H), 13.0 (s, 1H, exch with D₂O).

7,9-Dimethyl-4,4a,5,6-tetrahydrobenzo[h]cinnolin-3(2H)-one-2-acetic Acid (16c). The compound was prepared as reported above for the corresponding unsaturated term **2c**, starting from **21c,** through the ester **22c**.

22c: ^{1}H-NMR δ 1.2 (t, 3H, $J = 7$ Hz), 2.2 (2s, 6H), 2.3−3.0 (m, 4H), 4.1−4.2 (m, 4H), 4.6 (s, 2H), 7.0 (s, 1H), 7.8 (s, 1H).

16c: mp = 195–196 °C; ^{1}H-NMR δ 2.1 (2s, 6H), 2.2–3.0 (m, 6H), 4.6 (s, 2H), 7.0 (s, 1H), 7.8 (s, 1H). Anal. (C$_{16}$H$_{18}$N$_2$O$_3$) C, H, N.

Enzyme Section. Glutathione reductase type IV from yeast (100–300 U/mg), pyridine coenzymes, D,L-glyceraldehyde, glutathione disulfide, dithithreitol (DTT), sorbitol, D-glucuronate, and sodium valproate were purchased from Sigma Chemical Co. DEAE-cellulose (DE-52) was obtained from Whatman. Sephadex G75 resin was from Pharmacia Biotech. Orange Matrex A, centricon-10 microconcentrators, and YM10 ultrafiltration membranes were from Amicon. (*S*)-(+)-6-Fluoro-2,3-dihydrospiro(4*H*-1-benzopyran-4,4′-imidazolidine)-2′,5′-dione (sorbinil) was a gift from Pfizer (Groton, CT). Quercetin was purchased from Fluka Chemika. Sorbitol dehydrogenase from sheep liver (40 U/mg of protein) was from Boehringer Mannheim. All other chemicals were of reagent grade. Protein concentration was determined according to the method of Bradford,[36] using bovine serum albumin as standard. In order to minimize cross-contamination between ALR2 and ALR1 in the enzyme preparations used to test the susceptibility of both enzymes to inhibition, bovine lens, which contains a significantly high proportion of ALR2 over ALR1, and bovine kidney, in which ALR1 is the predominant enzyme,[37] were selected for isolation of ALR2 and ALR1, respectively. Calf lenses and kidneys for the purification of ALR2 and ALR1, respectively, were obtained locally from freshly slaughtered animals.

(a) Preparation of the Native and Modified Forms of ALR2. In order to purify the native form of bovine lens aldose reductase, the capsule was incised and the frozen lens was suspended in sodium potassium phosphate buffer, pH 7 (standard buffer), containing 5 mM DTT (1 g of tissue/3.5 mL) and stirred in an ice-cold bath for 1 h. The suspension was then centrifuged at 22000*g* at 4 °C for 40 min, and the supernatant was subjected to ion exchange chromatography on DE-52, affinity chromatography on Orange Matrex A, and Sephadex G75 chromatography, as previously described.[38] The pure native enzyme, which was stored at 4 °C in standard buffer supplemented with 2 mM DTT, exhibited a specific activity of 1.10 U/mg of protein. Partially purified enzyme preparations (i.e., after DE-52 chromatography) with a specific activity of 6.5 mU/mg were routinely used to test enzyme inhibition. No appreciable contamination by ALR1 could be detected, as evidenced by the K_m value of 25.1 ± 1.9 mM for D-glucose determined for the enzyme and the rather high level of IC$_{50}$ of 61.7 (57.4–66.3) μM for valproate, an efficient inhibitor of ALR1.[37] At this stage of purification, ALR2 could be stored at −20 °C without loss of activity for at least 1 month.

The glutathione-modified form of ALR2 was prepared as previously described,[12] the pure native enzyme (0.12 mg/mL) being incubated at 37 °C in standard buffer in the presence of 1.5 mM glutathione disulfide. After 2.5 h of incubation, the enzyme was dialyzed on Amicon YM10 membrane against the same buffer, concentrated to 0.2 mg/mL protein, and stored at 4 °C until used (no more than 5–7 days). The enzyme preparation contained 80% of modified ALR2 with a specific activity of 0.05 mU/mg of protein. The 2-mercaptoethanol-modified form of ALR2 was obtained as previously described[39] by incubating the native enzyme (0.03 mg/mL) in 50 mM sodium phosphate, pH 6.8, containing 5 mM 2-mercaptoethanol, 0.1 mM FeSO$_4$, and 0.3 mM EDTA. The modification process was monitored by measuring the activity of ALR2 at different times. After 2.5 h of incubation the enzyme preparation was dialyzed by Amicon YM10 membrane against standard buffer and concentrated to approximately 1 mg/mL. The specific activity of the modified form was 2.2 U/mg. Carboxymethylation of ALR2 was obtained by incubating the native enzyme (0.1 mg/mL) at 25 °C for 2.5 h in standard buffer supplemented with 5 mM iodoacetamide. After modification, the enzyme preparation was treated as described above for the 2-mercaptoethanol-modified form. The specific activity of the carboxymethylated enzyme was 2.4 U/mg.[25]

(b) Preparation of ALR1. Partially purified ALR1 was obtained following a previously reported method.[37] Bovine kidneys were homogenized in 3 vol of 0.25 M sucrose, 2.0 mM EDTA dipotassium salt, and 2.5 mM β-mercaptoethanol in 10 mM sodium phosphate buffer, pH 7.2 (S-buffer). The homogenate was centrifuged (16.000*g* for 20 min at 4 °C) and the supernatant subjected to ammonium sulfate fractional precipitation. The pellet obtained between 45% and 75% of salt saturation, containing ALR1 activity, was redissolved in S-buffer containing 2.0 mM EDTA (dipotassium salt) and 2.0 mM β-mercaptoethanol at a protein concentration of approximately 20 mg/mL. DEAE-52 resin was added to the solution and then removed by centrifugation; the supernatant was then stored at −20 °C. The enzyme preparation at this step of purification displayed a specific activity of 11.3 mU/mg and appeared devoid of any ALR2 activity, being ineffective in reducing glucose (up to 150 mM D-glucose used as substrate) and displaying an IC$_{50}$ for valproate of 2.01 (1.37–2.93) μM.[37] The enzyme can be stored at −20 °C without loss of activity for at least 1 month.

(c) Enzyme Activity Measurements. Enzyme activity for all tested enzymes was measured by monitoring the change in absorbance at 340 nm which accompanies the oxidation of NADPH or the reduction of NAD$^+$ catalyzed by ALR2, ALR1, GR, and SD, respectively. One unit of enzyme activity for all the tested enzymes is the amount of the enzyme which catalyzes the oxidation or the reduction of 1 μmol of the appropriate pyridine cofactor/min in the specified assay conditions. The assay for ALR2 activity was performed at 37 °C as previously described,[40] using 4.7 mM D,L-glyceraldehyde as substrate in 0.25 M sodium phosphate buffer, pH 6.8, containing 0.38 M ammonium sulfate and 0.11 mM NADPH. ALR1 activity was assayed at 37 °C using 20 mM D-glucuronate as substrate and 0.12 mM NADPH in 0.1 M sodium phosphate buffer, pH 7.2.[30] Sorbitol dehydrogenase activity was determined at 25 °C in 50 mM sodium phosphate buffer, pH 7.0, using 10 mM sorbitol as substrate and 0.47 mM NAD$^+$.[41] Glutathione reductase activity was assayed at 30 °C in 0.125 M sodium phosphate buffer, pH 7.4, supplemented by 6.3 mM potassium EDTA, in the presence of 0.3 mM glutathione disulfide and 0.36 mM NADPH.[42]

(d) Enzyme Inhibition. The sensitivity of the enzymes to inhibition by different ARIs and newly synthesized compounds was tested in the above assay conditions by including the inhibitor dissolved in DMSO at the desired concentration in the reaction mixture. DMSO in the assay mixture was kept at a constant concentration of 1%. A reference blank containing all the above reagents except the substrate was used to correct for the nonenzymatic oxidation of NADPH. The enzyme concentrations in the inhibition studies were as follows: 3.5 mU/mL for ALR2 and ALR1, 3.75 mU/mL for SD, and 4.5 mU/mL for GR. IC$_{50}$ values (the concentration of the inhibitor required to produce 50% inhibition of the enzyme-catalyzed reaction) were determined from least-squares analyses of the linear portion of the log dose–inhibition curves. Each curve was generated using at least three concentrations of inhibitor causing an inhibition between 20% and 80% with two replicates at each concentration. The 95% confidence limits (95% CL) were calculated from *T* values for $n - 2$, where *n* is the total number of determinations.[43]

Computational Procedure. Molecular mechanics and molecular dynamics calculations were performed using the AMBER all-atom force field and the AMBER 4.0 programs[44] running on a DEC-Alpha OSF/1 computer. Graphic display and manipulation were performed using MIDAS[45] on SGI computers at the Centro Interdipartimentale di Calcolo Elettronico of the University of Modena, Italy.

(a) Protein Structure. Because the crystal structure of bovine lens ALR2 (here used for the inhibition assays) is not known, calculations were performed starting from the coordinates of the human ALR2 holoenzyme;[28] however, the two sequences have 88% homology, and residues constituting the active site are highly conserved. One of the most potent inhibitors here developed, compound **8aa** in Table 1, was docked into the active site of the human holoenzyme; the carboxylate of **8aa** was initially positioned to interact with the nicotinamidic ring of NADP$^+$ and with the nearby residues, as indicated by the binding of zopolrestat to human ALR2.[13] The side-chain atoms of Asn129 are not included in the X-ray structure owing to disorder; they were generated using the

AMBER internal coordinate data base. Hydrogens were added to the protein using the stored internal coordinates of the AMBER all-atom data base and then minimized, the heavy atoms of the protein being kept fixed in their original positions. All Lys and Arg residues were positively charged and Glu and Asp residues negatively charged; the δH, ϵH, or protonated forms of histidines were assigned on the basis of favorable interactions with their environments. In order to neutralize the protein, counterions (Na$^+$, Cl$^-$) were placed around charged residues of the protein surface, and their position was optimized; the parameters for the Na$^+$ and Cl$^-$ counterions were taken from the works of Åqvist[46] and Jorgensen,[47] respectively. Water molecules buried inside the protein were maintained in the initial structure of ALR2, and the active site was further solvated with a spherical cap of 358 TIP3P[48] water molecules within 20 Å of the center of mass of the inhibitor. Harmonic radial forces (1.5 kcal/mol Å^2) were applied to avoid evaporation.

(b) NADP$^+$ and Inhibitor Structures. The oxidized form of NADPH (NADP$^+$) was used in all simulations because inhibitors preferentially bind to this form;[49] moreover, NADP$^+$ is the crystal-bound form of the cofactor.[23] The initial geometry of the inhibitor was built and then optimized with the AM1[50] Hamiltonian using MOPAC.[51] The carboxylate of the inhibitor was taken as dissociated. The atomic charges of the oxidized nicotinamide ring and the inhibitor, not included in the AMBER force field, were calculated from an electrostatic potential fit[52] to a STO-3G *ab-initio* wave function.

(c) Molecular Mechanics/Dynamics. The energy minimization of the ALR2 inhibitor complex was performed by optimizing the water molecules first, the protein, NADP$^+$, and the inhibitor being kept frozen. Next, all the residues within 15 Å of each atom of the inhibitor and all the water molecules were allowed to move; this selection resulted in 138 protein residues; 15 000 steps of minimization were performed with molecular mechanics, and the root-mean-square value of the potential gradients was <0.1 kcal/mol Å. A residue-based cutoff of 12 Å was employed. Molecular dynamics was performed for 180 ps. To this end, Cartesian coordinate restraints were applied during heating to 300 K and then gradually removed (first 2 ps) in order to reduce the initial atomic velocities. During dynamics, all bond lengths were constrained using the SHAKE[53] algorithm, allowing a time step of 2 fs. Solute and solvent were coupled to a constant temperature heat bath with a coupling constant of 0.2 ps to maintain the temperature at 300 K.

References

(1) Kador, P. F. The role of aldose reductase in the development of diabetic complications. *Med. Res. Rev.* **1988**, *8*, 325–352.

(2) Tomlinson, D. R.; Stevens, E. J.; Diemel, L. T. Aldose reductase inhibitors and their potential for the treatment of diabetic complications. *Trends Pharmacol. Sci.* **1994**, 293–297.

(3) Klopman, G.; Buyukbingol, E. An artificial intelligence approach to the study of the structural moieties relevant to drug-receptor interaction in aldose reductase inhibitors. *Mol. Pharmacol.* **1988**, *34*, 852–862.

(4) Butera, J.; Bagli, J.; Doubleday, W.; Humber, L.; Treasurywala, A.; Loughney, D.; Sestanj, K.; Millen, J.; Sredy, J. Computer-assisted design and synthesis of novel aldose reductase inhibitors. *J. Med.Chem.* **1989**, *32*, 757–765.

(5) Lee, Y. S.; Pearlstein, R.; Kador, P. F. Molecular modeling studies of aldose reductase inhibitors. *J. Med.Chem.* **1994**, *37*, 787–792.

(6) Dvornik, D. In *Aldose reductase inhibition. An approach to the prevention of diabetic complications*; Porte, D., Ed.; McGraw-Hill: New York, **1987**.

(7) Carper, D.; Wistow, G.; Nishimura, C.; Graham, C.; Watanabe, K.; Fuji, Y.; Hayashi, H.; Hayaishi, O. A Superfamily of NADPH-dependent reductases in eukaryotes and prokaryotes. *Exp. Eye Res.* **1988**, *49*, 377–388.

(8) Du Priest, M. T.; Griffin, B. W.; Kuzmich, P.; McNatt, L. G. Spiro[fluoreneisothiazolidin]one dioxide: new Aldose reductase and L-Hexonate dehydrogenase inhibitors. *J. Med. Chem.* **1991**, *34*, 3229–3234.

(9) Sarges, R.; Oates, P. J. Aldose reductase inhibitors: recent developments. *Prog. Drug Res.* **1993**, *40*, 99–161.

(10) Bhatnagar, A.; Srivastava, S. K. Review: Aldose reductase: congenial and injurious profiles of an enigmatic enzyme. *Biochem. Med. Metab. Biol.* **1992**, *48*, 91–121.

(11) Cappiello, M.; Vilardo, P. G.; Cecconi, I.; Leverenz, V.; Giblin, F. J.; Del Corso, A.; Mura, U. Occurrence of glutathione-modified aldose reductase in oxidatively stressed bovine lens. *Biochem. Biophys. Res. Commun.* **1995**, *207*, 775–782.

(12) Cappiello, M.; Voltarelli, M.; Giannessi, M.; Cecconi, I.; Camici, G.; Manao, G.; Del Corso, A.; Mura, U. Glutathione-dependent modification of bovine lens aldose reductase. *Exp. Eye Res.* **1994**, *58*, 491–501.

(13) Wilson, D. K.; Tarle, I.; Petrash, J. M.; Quiocho, F. A. Refined 1.8Å structure of human aldose reductase complexed with the potent inhibitor zopolrestat. *Proc. Natl. Acad. Sci. U.S.A.* **1993**, *90*, 9847–9851.

(14) Mylari, B. L.; Beyer, T. A.; Scott, P. J.; Aldinger, C. E.; Dee, M. F.; Siegel, T.W.; Zembrowski, W. J. Potent, orally active aldose reductase inhibitors related to Zopolrestat: surrogates for benzothiazole side chain. *J. Med. Chem.* **1992**, *35*, 457–465.

(15) Mylari, B. L.; Zembrowski, W. J.; Beyer, T. A.; Aldinger, C. E.; Siegel, T. W. Orally active aldose reductase inhibitors: indazoleacetic, oxopyridazineacetic and oxopyridopyridazineacetic acid derivatives. *J. Med. Chem.* **1992**, *35*, 2155–2162.

(16) Coudert, P.; Albuisson, E.; Boire, J. Y.; Duroux, E.; Bastide, P.; Couquelet, J. Synthesis of pyridazine acetic acid derivatives possessing aldose reductase inhibitory activity and antioxidant properties. *Eur. J. Med. Chem.* **1994**, *29*, 471–477.

(17) Cignarella, G.; Barlocco, D.; Pinna, G. A.; Loriga, M.; Tofanetti, O.; Germini, M.; Sala, F. Conformationally restricted congeners of hypotensive and platelet agggregation inhibitors: 6-aryl-5-methyl-4,5-dihydro-3(2H)-pyridazinones derived from 5H-indeno[1,2-c]pyridazine. *J. Med. Chem.* **1986**, *29*, 2191–2194.

(18) Cignarella, G.; Barlocco, D.; Pinna, G. A.; Loriga, M.; Curzu, M. M.; Tofanetti, O.; Germini, M.; Cazzulani, P.; Cavalletti, E. Synthesis and biological evaluation of substituted benzo[h]-cinnolinones and 3H-benzo[6,7]cyclohepta[1,2-c]pyridazinones: higher homologues of the antihypertensive and antithrombotic 5H-indeno[1,2-c]pyridazinones. *J. Med. Chem.* **1989**, *32*, 2277–2282.

(19) Giblin, F. J.; Mc Cready, J. P.; Schrimscher, L.; Reddy, V. N. Peroxide-induced effects on lens cation transport following inhibition of glutathione reductase activity *in vitro*. *Exp. Eye Res.* **1987**, *45*, 77–91.

(20) Reddan, J. R.; Giblin, F. J.; Dziedzic, D. C.; Mc Cready, J. P.; Schrimscher, L.; Reddy, V. N. Influence of the activity of glutathione reductase on the response of cultured lens epithelial cells from young and old rabbits to hydrogen peroxide. *Exp. Eye Res.* **1988**, *45*, 209–221.

(21) Singh, B.; Lesher, G. Y. Synthesis of aza analogs of amrinone. *Heterocycles* **1990**, *31*, 2163.

(22) Petrash, J. M.; Tarle, I.; Wilson, D. K.; Quiocho, F. A. Aldose reductase catalysis and crystallography. Insights from recent advances in enzyme structure and function. *Diabetes* **1994**, *43*, 955–959.

(23) Harrison, D. H.; Bohren, K. M.; Ringe, D.; Petsko, G. A.; Gabbay, K. H. An anion binding site in human aldose reductase: mechanistic implications for the binding of citrate, cacodylate, and glucose-6-phosphate. *Biochemistry* **1994**, *33*, 2011–2020.

(24) Kook, P. N.; Ward, W. H. J.; Petrash, J. M.; Mirrlees, D. J.; Serenitt, C. M.; Carey, F.; Preston, J.; Brittain, D. R.; Tuffin, D. P.; Lowe, R. Kinetic characteristics of Zeneca ZD5522, a potent inhibitor of human and bovine lens aldose reducatse. *Biochem. Pharmacol.* **1995**, *49*, 1043–1049.

(25) Liu, S. Q.; Bhatnagar, A.; Ansari, N. H.; Srivastava, S. K. Identification of the reactive cysteine residue in human placenta aldose reductase. *Biochim. Biophys. Acta* **1993**, *1164*, 268–272.

(26) Del Corso, A.; Barsacchi, D.; Giannessi, M.; Tozzi, M. G.; Houben, J. L.; Zandomeneghi, M.; Camici, M.; Mura, U. Kinetic and structural properties of the native and oxidatively modified forms of bovine lens aldose reductase. In *Current Concepts of Aldose Reductase and its Inhibition*; Sakamoto, N., et al., Eds.; Elsevier: Amsterdam, **1990**; pp 195–198.

(27) Bohren, K. M.; Gabbay, K. H. Cys298 is responsible for reversible thiol-induced variation in aldose reductase activity. In *Enzymology and Molecular Biology of Carbonyl Metabolism 4*; Weiner, H., Ed.; Plenum Press: New York, 1993; pp 267–277.

(28) Wilson, D. K.; Bohren, K. M.; Gabbay, K. H.; Quiocho, F. A. An unlikely sugar substrate site in the 1.65Å structure of the human

aldose reductase holoenzyme implicated in diabetic complications. *Science* **1992**, *257*, 81−84.

(29) Bohren, K. M.; Grimshaw, C. E.; Lai, C. J.; Harrison, D. H.; Ringe, D.; Petsko, G. A.; Gabbay, K. H. Tyrosine-48 is the proton donor and histidine-110 directs substrate stereochemical selectivity in the reduction reaction of human aldose reductase: enzyme kinetics and crystal structure of the Y48H mutant enzyme. *Biochemistry* **1994**, *33*, 2021−2032.

(30) Bhatnagar, A.; Liu, S. Q.; Ueno, N.; Chakrabarti, B.; Srivastava, S. K. Human placental aldose reductase: role of Cys298 in substrate and inhibitor binding. *Biochim. Biophys. Acta* **1994**, *1205*, 207−214.

(31) Cappiello, M.; Voltarelli, M.; Cecconi, I.; Vilardo, P. G.; Dal Monte, M.; Marini, I.; Del Corso, A.; Petrash, J. M.; Mura, U. Specifically targeted modification of human aldose reductase by physiological disulfides. *J. Biol. Chem.*, in press.

(32) Howard, A. E.; Kollman, P. A. Molecular dynamics studies of a DNA-binding protein: 1. A comparison of the trp repressor and trp aporepressor aqueous simulations. *Protein. Sci.* **1992**, *1*, 1173−1184.

(33) Guenot, J.; Kollman, P. A. Molecular dynamic studies of a DNA-binding protein: 2. An evaluation of implicit and explicit solvent models for the molecular dynamics simulation of the Escherichia Coli trp repressor. *Protein. Sci.* **1992**, *1*, 1185−1205.

(34) Miyamoto, S.; Kollman, P. A. Absolute and relative binding free energy calculations of the interaction of biotin and its analogues with strepavidin using molecolar dynamics/free energy perturbation approaches. *Proteins: Struct., Funct., Genet.* **1993**, *16*, 226−245.

(35) Sestany, K.; Bellini, F.; Fung, S.; Abraham, N.; Treasurywala, A.; Humber, L.; Duquesne, N. S.; Dvornik, D. N-[[5-(trifluoromethyl)-6-methoxy-1-naphthalenyl]thioxomethyl]-N-methylglycine (Tolrestat), a potent, orally active Aldose Reductase Inhibitor. *J. Med. Chem.* **1984**, *27*, 255−256.

(36) Bradford, M. M. A rapid and sensitive method for the quantitation of microgram quantities of protein utilizing the principle of protein-dye binding. *Anal. Biochem.* **1976**, *72*, 248−250.

(37) Ward, W. H. J.; Sennitt, C. M.; Ross, H.; Dingle, A.; Timms, D.; Mirrlees, D. J.; Tuffin, D. P. Ponalrestat: a potent and specific inhibitor of aldose reductase. *Biochem. Pharmacol.* **1990**, *39*, 337−346.

(38) Del Corso, A.; Barsacchi, D.; Giannessi, M.; Tozzi, M. G.; Camici, M.; Houben, J. L.; Zandomeneghi, M.; Mura, U. Bovine lens aldose reductase: tight binding of the pyridine coenzyme. *Arch. Biochem. Biophys.* **1990**, *283*, 512−518.

(39) Giannessi, M.; Del Corso, A.; Cappiello M.; Marini, I.; Barsacchi, D.; Garland, D.; Camici, M.; Mura, U. Thiol-dependent metal catalyzed oxidation of bovine lens aldose reductase I. Studies on the modification process. *Arch. Biochem. Biophys.* **1993**, *300*, 423−429.

(40) Del Corso, A.; Camici M.; Mura U. In vitro modification of bovine lens aldose reductase activity. *Biochem. Biophys. Res. Commun.* **1987**, *148*, 369−375.

(41) Lindstad, R. I.; Hermansen, L. F.; McKinley-McKee, J. S. Inhibition and activation studies on sheep liver sorbitol dehydrogenase. *Eur. J. Biochem.* **1994**, *221*, 847−854.

(42) Fitzgerald, G. B.; Bauman, C.; Sajjat Hussoin, Md.; Wick, M. M. 2,4-Dihydroxybenzylamine: a specific inhibitor of glutathione reductase. *Biochem. Pharmacol.* **1991**, *41*, 185−190.

(43) Tallarida, R. J.; Murray, R. B. *Manual of Pharmacologic calculations with computer programs*, 2nd ed.; Springer Verlag: New York, 1987.

(44) Pearlman, D. A.; Case, D. A.; Caldwell, J. A.; Seibel, G. L.; Singh, U. C.; Weiner, P.; Kollman, P. A. *AMBER 4.0*; University of California: San Francisco, 1991.

(45) Ferrin, T. E.; Huang, C. C.; Jarvis, L. E.; Langridge, R. The MIDAS display system. *J. Mol. Graph.* **1988**, *6*, 13−27.

(46) Åqvist, J. Water interaction potentials derived from free energy perturbation simulations. *J. Phys. Chem.* **1990**, *94*, 8021−8024.

(47) Jorgensen, W. L.; Buckner, J. K.; Huston, S. E.; Rossky, P. J. Hydration and energetics for $(CH_3)_3CCl$ ion pairs in aqueous solution. *J. Am. Chem. Soc.* **1987**, *109*, 1891−1899.

(48) Jorgensen, W. L.; Chandrasekhar, J.; Madura, J. D.; Impey, R. W.; Klein, M. L. Comparison of simple potential functions for simulating liquid water. *J. Chem. Phys.* **1983**, *79*, 926−935.

(49) Ehrig, T.; Bohren, K. M.; Prendergast, F. G.; Gabbay, K. H. Mechanism of aldose reductase inhibition: binding of $NADP^+$/NADPH and alrestatin-like inhibitors. *Biochemistry* **1994**, *33*, 7157−7165.

(50) Dewar, M. J. S.; Zoebisch, E. G.; Healey, E. F.; Stewart, J. J. P. AM1: A new general purpose quantum mechanical molecular model. *J. Am. Chem. Soc.* **1985**, *107*, 3902−3909.

(51) Stewart, J. J. P. MOPAC 6.0. *QCPE 455*.

(52) Singh, U. C.; Kollman, P. A. An approach to computing electrostatic charges for molecules. *J. Comput. Chem.* **1984**, *5*, 129−144.

(53) van Gunsteren, W. F.; Berendsen, H. J. C. Algorithms for macromolecular dynamics and constraint dynamics. *Mol. Phys.* **1977**, *34*, 1311−1327.